Cell, Vol. 106, 417–428, August 24, 2001, Copyright ©2001 by Cell Press

Mechanism of Processivity Clamp Opening by the Delta Subunit Wrench of the Clamp Loader Complex of *E. coli* DNA Polymerase III

David Jeruzalmi, Olga Yurieva, Yanxiang Zhao, Matthew Young, Jelena Stewart, Manju Hingorani, Mike O'Donnell, and John Kuriyan[1]
Howard Hughes Medical Institute
The Rockefeller University
1230 York Avenue
New York, New York 10021

Summary

The dimeric ring-shaped sliding clamp of *E. coli* DNA polymerase III (β subunit, homolog of eukaryotic PCNA) is loaded onto DNA by the clamp loader γ complex (homolog of eukaryotic Replication Factor C, RFC). The δ subunit of the γ complex binds to the β ring and opens it. The crystal structure of a β:δ complex shows that δ, which is structurally related to the δ′ and γ subunits of the γ complex, is a molecular wrench that induces or traps a conformational change in β such that one of its dimer interfaces is destabilized. Structural comparisons and molecular dynamics simulations suggest a spring-loaded mechanism in which the β ring opens spontaneously once a dimer interface is perturbed by the δ wrench.

Introduction

DNA polymerases that replicate chromosomes require multiple accessory proteins for the processive synthesis of DNA (Huang et al., 1981; Kornberg and Baker, 1991). In the *E. coli* DNA replication system, one of these accessory proteins forms a topological link to DNA (the β clamp) and the other accessory proteins function as a clamp loader complex that couples ATP binding and hydrolysis to the assembly of the β clamp on DNA (Stukenberg et al., 1991). The β subunit is a ring with a central cavity that is sufficiently large to encircle duplex DNA without steric hindrance, and is formed from two crescent-shaped protomers (Kong et al., 1992). The β clamp slides on DNA and tethers the catalytic subunits of the polymerase to the template. This mechanism, in which a polymerase with low intrinsic affinity for DNA is made highly processive by attachment to a DNA-encircling platform has been conserved throughout evolution (Hingorani and O'Donnell, 2000; Kelman and Hurwitz, 2000; Stillman, 1994; Young et al., 1992).

Replication of chromosomal DNA in *E. coli* is carried out by DNA polymerase III holoenzyme, which contains three subassemblies (Kelman and O'Donnell, 1995). The catalytic core (subunits α, ε, and θ) is responsible for DNA synthesis and proofreading. The sliding clamp (β subunit) provides processivity. The clamp loader (γ complex, subunits γ, δ, δ′, χ, and ψ; the last two are not essential for clamp loading and are not included in subsequent discussion) is required for loading the sliding clamp (β) onto DNA. In T4 and related bacteriophages, such as RB69, the sliding clamp protein is gp45, and the clamp loader complex consists of the gp44 and gp62 proteins (Young et al., 1992). In eukaryotes, the sliding clamp is the PCNA (proliferating cell nuclear antigen) protein, and five clamp loader subunits form a complex known as RFC (Replication Factor C) (Stillman, 1994). Archaebacteria have two clamp loader subunits that are closely related to the eukaryotic RFC subunits (Kelman and Hurwitz, 2000), as well as a clamp that is similar to eukaryotic PCNA (Matsumiya et al., 2001).

The bacterial sliding clamp is composed of two β monomers arranged head to tail in a circular dimer (Kong et al., 1992). Each monomer contains three domains with identical chain topology (Domains 1, 2, 3). Eukaryotic PCNA and T4 gp45 are strikingly similar in structure to the β clamp, but are trimers that have two rather than three domains in each protomer (Gulbis et al., 1996; Krishna et al., 1994; Moarefi et al., 2000; Shamoo and Steitz, 1999).

β subunit is very stable as a dimer ($K_d < 50$ nm), and the half life of a β ring on DNA is ~100 min at 37°C (Leu et al., 2000; Yao et al., 1996). The elements that stabilize the β ring include a β sheet that is continuous across each dimer interface, as well as an array of hydrophobic and electrostatic interactions (Kong et al., 1992). Because of the stability of the dimer, efficient assembly of the sliding clamp on DNA requires ATP and the γ complex (defined here as an assembly of γ, δ, and δ′ that is active in clamp loading). The γ subunit is the ATPase motor (Tsuchihashi and Kornberg, 1989), while the δ′ subunit is an inert stator, and both are members of the AAA+ family of ATPases (Neuwald et al., 1999). Structural analysis shows that the stoichiometry of the γ complex is $\gamma_3\delta\delta'$ (see accompanying paper, Jeruzalmi et al., 2001 [this issue of *Cell*]).

Of the three unique subunits of the γ complex, δ is the only one that is capable of binding to and opening the β clamp on its own (Turner et al., 1999). In the absence of ATP, the γ complex interacts only weakly with the β clamp, suggesting that δ is somehow sequestered within the clamp loader (Naktinis et al., 1995). That ATP binding releases the crucial elements of δ is inferred from the ability of ATP-bound clamp loader complex to bind to the β clamp as strongly as isolated δ subunit (Hingorani and O'Donnell, 1998; Naktinis et al., 1995). The addition of primed DNA to a clamp loader–clamp complex stimulates the ATPase activity of the γ subunit substantially (Hingorani and O'Donnell, 1998; Onrust et al., 1991). Hydrolysis of ATP causes δ to be inaccessible again, with the release of the sliding clamp on DNA (Turner et al., 1999).

We have studied the mechanism by which the δ subunit opens the β ring by determining the structure of a β:δ complex. Our crystallographic results show that the chain fold of δ is essentially the same as that seen previously for the δ′ subunit, despite the lack of significant sequence identity between these two proteins. The structure of the β:δ complex indicates that there are two components to the mechanism by which the interaction with δ results in the opening of the β ring. δ acts as a

[1] Correspondence: kuriyan@rockefeller.edu

wrench in that it induces or traps a conformational change in β at its dimer interface such that ring closure is no longer supported. Additionally, the curvature of the β monomer is reduced in the β:δ complex relative to that of the β monomer in the β dimer. Molecular dynamics simulations indicate that this opening up of the β monomer results from an intrinsic tendency of β to adopt a more open conformation than that seen in the dimeric ring. There is, as a consequence, a spontaneous spring-loaded component to the ring opening mechanism that supplements the action of the δ wrench.

Results and Discussion

Structure Determination

Crystallization attempts using wild-type β and full-length δ were unsuccessful. We therefore turned to a form of β that is primarily monomeric in solution, as a result of replacement by alanine of two hydrophobic residues on Domain 3 at the dimer interface (Ile-272 and Leu-273) (Stewart et al., 2001). This monomeric β interacts with δ at least 50-fold more tightly than does wild-type β, and was crystallized in complex with two forms of δ. First, full-length wild-type δ was crystallized in a 1:1 complex with mutant β. This crystal form has two copies of the β:δ complex in the asymmetric unit, and the structure has been determined at 2.9 Å resolution. Analysis of the structure showed that only the N-terminal domain of δ (residues 1 to 140) makes contact with β. A truncated form of δ (δ^{1-140}, residues 1 to 140) was crystallized in a 1:1 complex with β. The structure of the β:δ^{1-140} complex has been determined at 2.5 Å resolution and was used for a detailed analysis of the interface.

The Fold of the δ Subunit Is Similar to that of Other Clamp Loader Subunits and AAA+ ATPases

δ consists of three separable domains, each of which is closely related to a corresponding domain in the δ′ stator, the only clamp loader subunit whose structure was known previously (Guenther et al., 1997). An N-terminal domain (Domain I, residues 1 to 140) consists of a central six-stranded β sheet surrounded by five α helices, and has a RecA-like fold that resembles that of many nucleotide binding domains. A core region of 64 residues can be superimposed between δ and δ′, with an rms deviation in Cα positions of 1.8 Å. A zinc binding module (of unknown function), present in the structures of δ′ and γ, is absent in δ.

Domain II (residues 141–210) is a four-helix bundle that is slightly larger than its counterparts in δ′ and γ because of an additional 2-stranded β sheet and an extra helix (Figure 1). Domain III (residues 211–343) also has an additional helix, but is otherwise similar to δ′. Domains I and II together resemble the core structures of AAA+ ATPases, many of which form hexameric assemblies containing a single type of subunit, such as the NSF protein that is involved in vesicle fusion (Lenzen et al., 1998; Yu et al., 1998) (reviewed in May et al. (2001)). The linker between Domain II and Domain III is flexible. The structure of δ in the γ complex (see accompanying paper, Jeruzalmi et al., 2001) differs from that in the β:δ complex in that Domain III is rotated by ~90° with respect to the orientation seen in either of the two molecules in the asymmetric unit of the β:δ crystals. An evolutionary relationship between δ′, γ, and the eukaryotic RFC subunits (Cullman et al., 1995; O'Donnell et al., 1993) was not extended previously to include the δ subunit because of its dissimilar sequence. Indeed, structural alignment of each of the domains of δ′ and δ shows that the level of sequence identity between them is only ~6%–8%. Nevertheless, the close structural correspondence between δ and δ′ makes it reasonable to assume that δ also derives from an ancestor that is common to all the clamp loader subunits.

A Conserved Hydrophobic Plug from δ Is Wedged into a Hydrophobic Crevice between Domains 2 and 3 of β

Of the three domains of δ, only the N-terminal domain (Domain I) is involved in interactions with β. The β-interaction elements on δ (helix α4 and the loops that flank it) are restricted to a region that is distal to the Domain I/Domain II connector (Figure 1). The interaction between δ and β is restricted to one face of the β ring, and does not involve the dimer interface directly (Figure 2). The head-to-tail nature of dimer formation results in the β subunit ring having two dissimilar faces, and δ binds to the face of β from which the C-terminal region of β protrudes (Figure 2). Consistent with the observed 1:1 stoichiometry of the β:δ complex in solution (Naktinis et al., 1995), only one molecule of δ can bind to a dimeric β assembly, because Domains II and III of δ are extended over the face of the ring (Figure 2).

When viewed along the edge of the central β sheet, the N-terminal domain of δ resembles a triangular wedge (Figure 2). The tip of this wedge is formed by the N-terminal ends of two adjacent β strands (β2 and β3), as well the loops preceding them. This tip of the Domain I wedge is inserted into a cleft between Domains 2 and 3 of the β subunit (Figure 3). The heart of the interface involves three hydrophobic residues of δ: Met-71, Leu-73, and Phe-74. Of these, Leu-73 and Phe-74 protrude out to form a hydrophobic plug that fits into a hydrophobic pocket on the surface of β, formed by Leu-177, Pro-242, Val-247, Val-36 and Met-362 (Figure 3). There is an additional interaction between δ and a loop in β (following helix α1″ in Domain 3 of β, using the notation of Kong et al. (1992)) that leads to an extensive restructuring of that loop (Figure 4A). This conformational change in β is important for the ring opening mechanism, as discussed below.

The β:δ interface buries ~1900 Å^2 of surface area spanning both molecules. On δ, the region of the surface that is most conserved involves Leu-73 and Phe-74, and these residues are responsible for the most highly conserved feature on the entire surface of δ. Likewise, the region of β that binds to δ forms an extended patch of highly conserved residues on the β surface (Figure 3).

The Interaction between δ and β Resembles the Binding of Anchor Segments of DNA Polymerase and the Inhibitor p21 to gp45 and PCNA

The central elements of the interaction between δ and β resemble very closely the manner in which the cell cycle protein p21/waf1/cip1 (p21) binds to PCNA (Gulbis et al., 1996), as well as the docking of a segment of

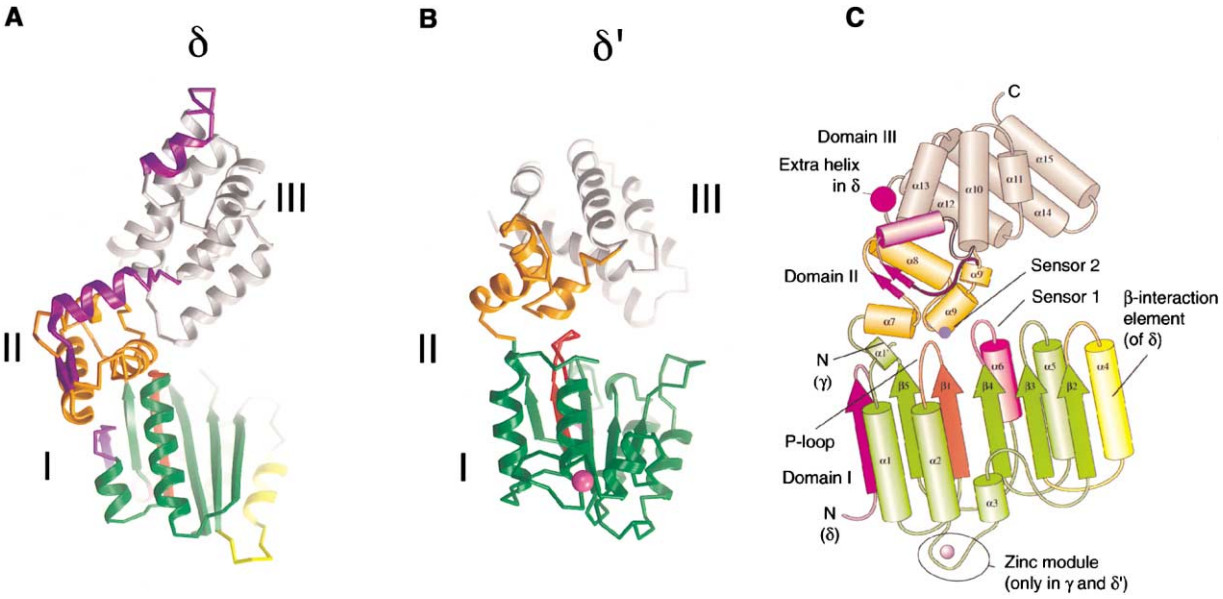

Figure 1. Structure of the δ Subunit

(A) A representation of the backbone structure of the δ subunit, from one of the structures of full-length wild-type δ bound to monomeric β. Domains I, II, and III are indicated. (B) Structure of the δ′ subunit, PDB code 1A5T (Guenther et al., 1997). (C) Schematic representation of the secondary structural elements of the clamp loader subunits δ, δ′, and γ (see accompanying paper, Jeruzalmi et al., 2001). Elements unique to δ are colored violet. Figures were composed using BOBSCRIPTv2.4 (Esnouf, 1997), GRASPv1.25 (Nicholls et al., 1991) and POVRAY v3.1 (http://www.povray.org), or MEGAPOVv0.5 (http://www.nathan.kopp.com/patched.htm).

the RB69 DNA polymerase onto the gp45 sliding clamp (Shamoo and Steitz, 1999). DNA polymerases that attach to sliding clamps do so by utilizing a short C-terminal extension that binds to the surface of the sliding clamp ring. p21, better known as an inhibitor of cyclin-dependent kinases, also has a C-terminal extension that binds to PCNA, except that in this case the interaction jams the works by preventing the eukaryotic polymerase δ from binding to PCNA (Flores-Rozas et al., 1994; Waga et al., 1994).

The interaction of p21 and the RB69 polymerase segment with their respective targets have two elements in common (Gulbis et al., 1996; Shamoo and Steitz, 1999). The N-terminal region of each peptide forms an extended structure that interacts with the very C-terminal residues of the clamp. A single turn of 3-10 helix follows, which presents three hydrophobic residues that plug into a hydrophobic crevice at the interdomain interface of their respective targets. These elements are mirrored by the interaction of δ with β. When β strands at the Domain 2-3 interface of β are aligned structurally with the interdomain region of PCNA and RB69 gp45, residues 69–75 of δ align very closely with the N-terminal portion and the beginning of the 3-10 helix of p21 and the RB69 polymerase segment (Figure 5). Particularly striking is the overlap of Leu-73 and Phe-74 of δ with leucine and phenylalanine side chains that are in precisely corresponding positions in the RB69 polymerase segment. p21 has a methionine and a threonine at the corresponding positions, and these have been shown to be critical for the ability of p21 to block PCNA function (Nakanishi, 1995; Warbrick, 1995).

It is remarkable that sliding clamps with such divergent sequences (there is no significant sequence similarity between β, PCNA, and gp45) all interact with a clamp loader (δ), an inhibitor (p21), and the RB69 DNA polymerase in such a similar way. This structural correspondence suggests strongly that the mechanisms for clamp opening and polymerase recruitment have been conserved across evolution.

Interaction with δ Requires Conformational Changes in β that Weaken the Dimer Interface

Although δ does not interact directly with the dimer interface in β, there are structural changes at the dimer interface that can be ascribed to the interaction with δ. Dimer formation in β involves an α helix (α1″) and a β strand at the edge of Domain 3 that pack against the corresponding elements of Domain 1 of the other β monomer in the dimer. In the structure of dimeric β, α1″ is distorted from ideal helical geometry, and this distortion is required for maintenance of the dimer interface. The last three residues of this helix (Ala-271, Ile-272, and Leu-273) are unwound and kinked so that the side chains of Ile-272 and Leu-273 fit into hydrophobic pockets on the surface of Domain 1 of the second β monomer.

In the structure of β in the β:δ complex, helix α1″ of Domain 3 (distorted in the structure of dimeric β) is essentially undistorted, and the Cα positions of residues 271, 272, and 273 are displaced by 1.6 Å, 2.5 Å, and 3.8 Å with respect to their positions in the dimeric β (measured after the structure of Domain 3, excluding helix α1″, is superimposed in the two structures). This prevents the formation of a well-packed dimer interface, because these side chains would collide with the surface of Domain 1 of the other β monomer (Figure 4A). A direct coupling between this structural distortion and the binding of δ to β is provided by the 5-residue loop

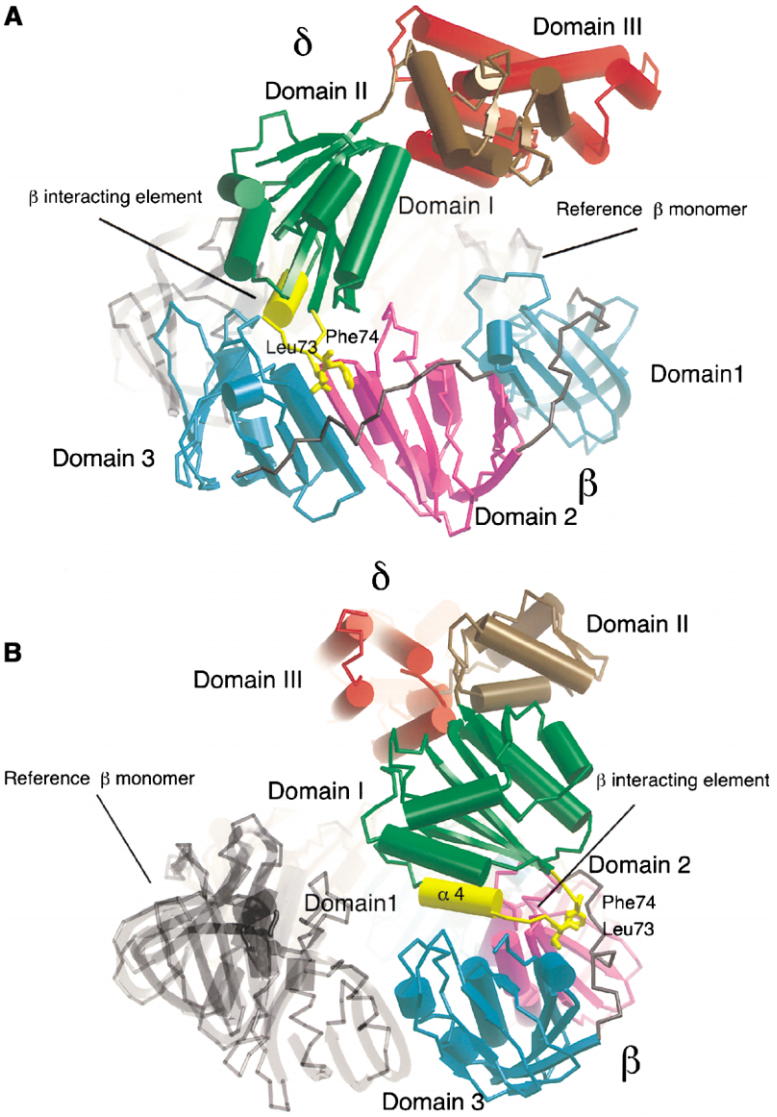

Figure 2. Structure of the β:δ Complex

(A) View along the edge of the β ring, centered on Domain 2 of β. (B) View showing the intermolecular interface involving Domain 3 of β. Structures shown in color are the β subunit and the δ subunit from the crystal structure of the complex. For reference, a second β monomer is shown in gray, taken from the crystal structure of the dimeric form of β (Kong et al., 1992), PDB code 2POL. The β-interaction element on δ (helix α4 and the loop following it) is colored yellow, and the side chains of two key hydrophobic residues of δ (Leu-73 and Phe-74) are shown.

in β that immediately follows helix α1″ (residues 274 to 278), which interacts closely with δ in the β:δ complex. In dimeric β, the structure of this loop is well-defined due to the presence of a β turn between residues 275 and 278, but its conformation would prevent the binding of δ. We surmise that alterations in the structure of this loop that are induced by δ impose strain on the distorted C-terminal end of helix α1″, and that this strain is released by relaxation of the helix into the more regular structure observed in the β:δ complex.

The β:δ Interface Involves a Reciprocal Induced Fit in δ

A prominent feature of δ in the β:δ complex is the extension away from the main body of Domain I of the hydrophobic plug that wedges into β (including Leu-73 and Phe-74). Comparison with the structure of δ in the γ complex (see accompanying paper, Jeruzalmi et al., 2001) shows that in the absence of β, the conformation of the β-interacting element of δ is dramatically different.

In going from the β-free to the β-bound form, helix α4 of δ translates by ~5.5 Å and rotates by ~45° about the helical axis with respect to the rest of Domain I. This rather large structural change includes complete rearrangement of the molecular interactions between the helix and the main body of δ. The last turn of the helix is completely unwound in the β:δ complex, allowing Leu-73 and Phe-74 to interact with β. The conformational change in going from the β-bound to the β-free form (seen in the γ complex structure) results in the exposure of two hydrophobic side chains on δ, Trp-61 and Phe-62 (Figure 4C). In the accompanying paper (Jeruzalmi et al., 2001), we discuss the potential role for these residues in an interaction with δ′ that might occur in the nucleotide-free state of the γ complex.

The rotation and translocation of helix α4 in δ is reminiscent of the action of a plumber's wrench that couples internal rotations to structural adjustments at the site of torque generation. While δ might actually function by trapping a transiently formed open conformation of β, rather than by inducing it directly, the analogy to a wrench appears to be apt.

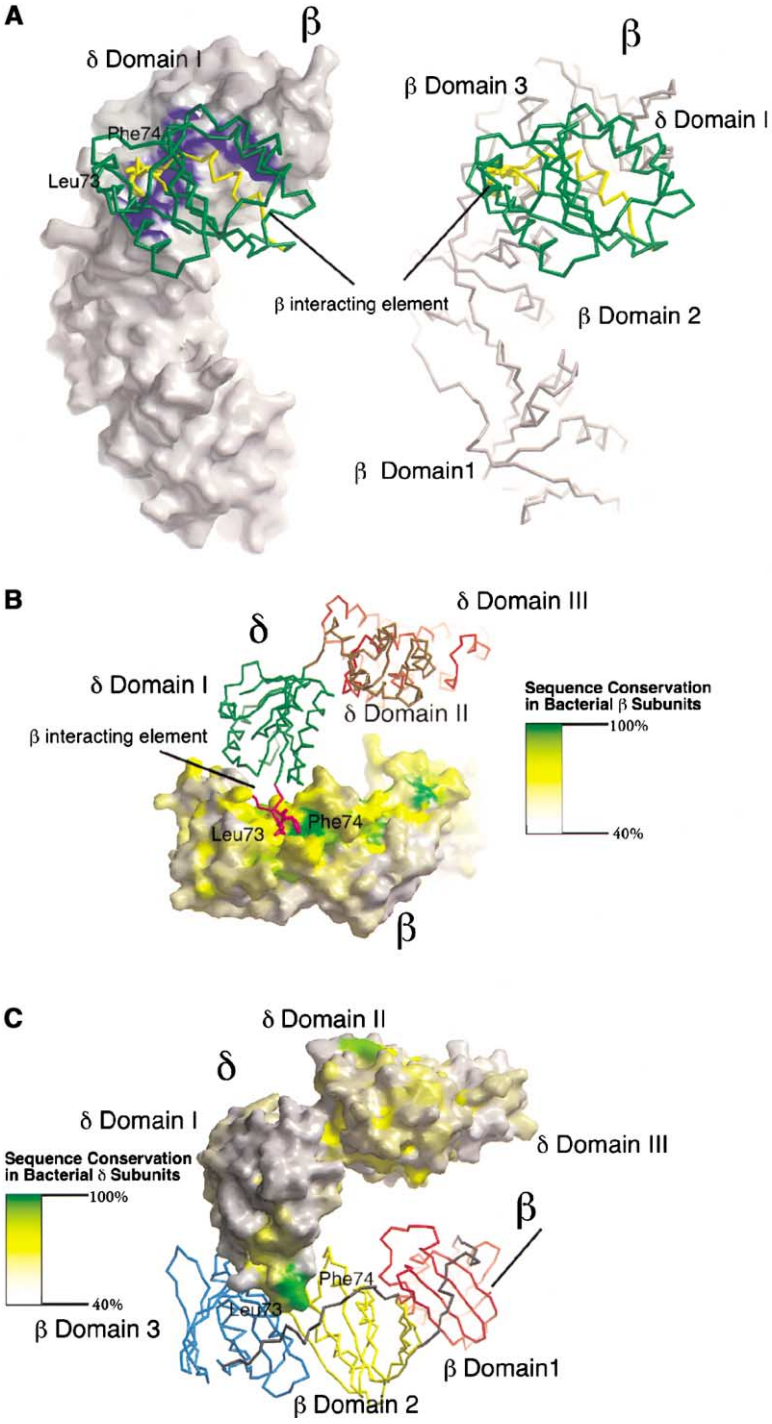

Figure 3. Features of the Interfacial Surface between β and δ

(A) The footprint of δ on β is shown in blue on the left, on the molecular surface of the β monomer. The backbone of Domain I of δ is shown in green, with the β-interaction element of δ colored yellow. The footprint of δ on β spans Domains 2 and 3 of β, as can be seen in the backbone representation of β on the right. (B) The surface of the β subunit in the β:δ complex, colored according to the sequence conservation of the underlying residues in an alignment of bacterial β subunits. The color scale runs from dark green for 100% conservation to white for 40% or less conservation. The structure of δ is shown in a backbone representation, with the β-interaction element of δ colored red. The binding surface on β for the hydrophobic residues of δ is highly conserved. (C) The surface of δ, colored as for β in (B). The hydrophobic residues that insert into the surface of β form a highly conserved surface feature.

The Structure of β in the β:δ Complex Has Reduced Curvature Relative to the Structure in the β Dimer

Superposition of Domain 2 of β from the structure of dimeric β (Kong et al., 1992) upon Domain 2 from the β:δ complex reveals a systematic distortion of β in all three independent crystallographic views of the β:δ complex. Domain 3 rotates outward by 5° in the β:δ complex, away from the central cavity. The change in Domain 1 is larger, and it rotates by ~12° away from the path followed by dimeric β. Crystal packing forces are unlikely to underlie these structural changes, since the packing around the 3 β:δ complexes is quite different and the conformation of the β monomers is the same in all three.

The extent of the structural change in β can be appreciated by superimposing two copies of the "relaxed" β structure (in the β:δ complex) upon the structure of the β ring. Disulfide cross-linking experiments show that only one of the two interfaces in dimeric β opens upon

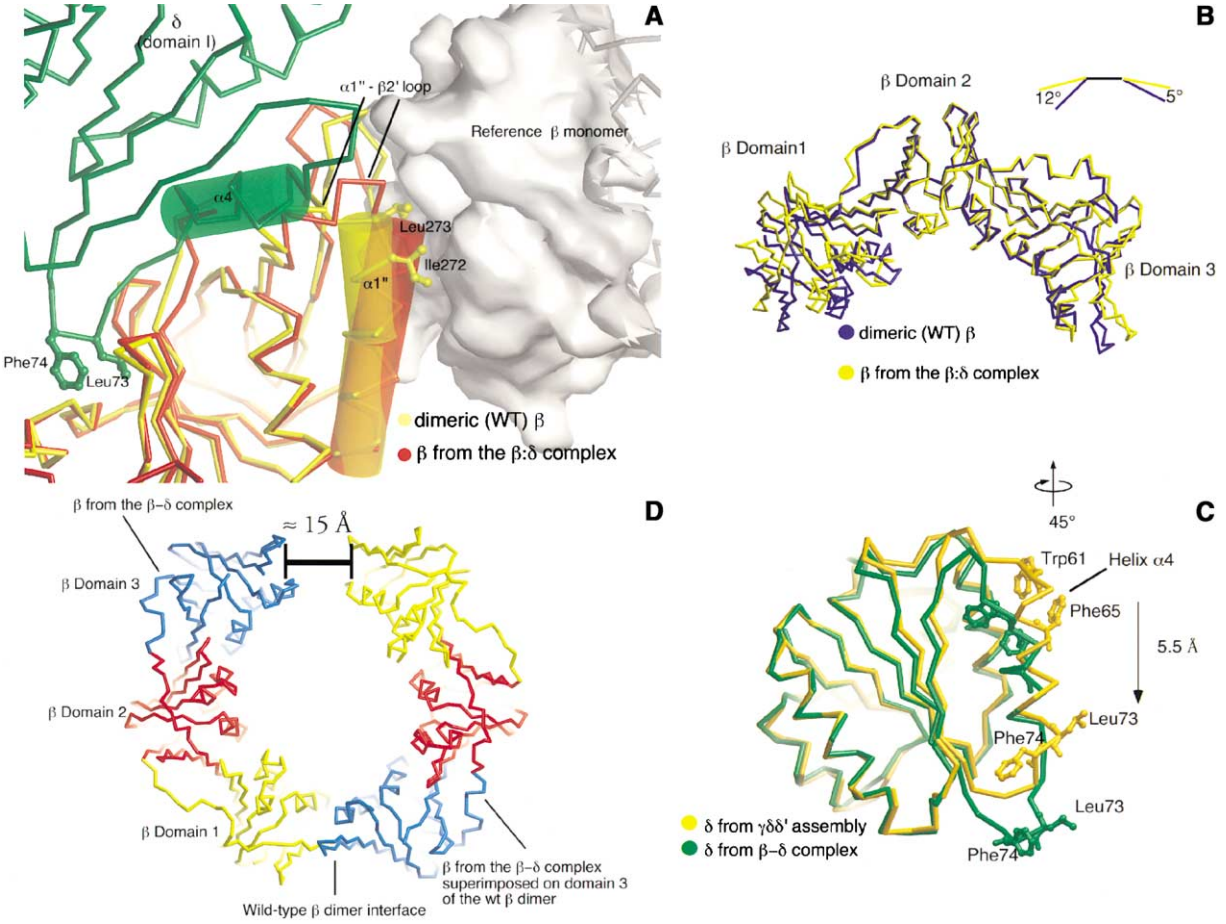

Figure 4. Conformational Changes in β and δ

(A) Conformational change in β at the dimer interface. The structure of Domain 3 of β is shown in yellow (dimeric form of β) and red (β monomer in the β:δ complex). Helix α1″, which is kinked in the dimeric form of β, is shown as a cylinder. Two hydrophobic side chains (Leu-273 and Ile-272) that are buried at the dimer interface and that are presented by this helix are shown. In the monomeric form of β, helix α1″ is straight, and the side chains at positions 273 and 272 would collide with the other monomer in the dimer. The α1″-β2 loop in the structure of dimeric β overlaps with the δ subunit in the structure of the β:δ complex, and it changes conformation, as indicated. (B) Change in overall curvature of β. The backbone structures of one subunit from the dimer (blue) and the β monomer in the β:δ complex (yellow) are shown, superimposed on Domain 2. (C) Structural change in the β-interaction element of δ. Helix α4 of δ rotates by ~45° about its axis, translocates downward by ~5.5 Å, and changes the nature of its packing with the main body of Domain I of δ as it converts from the β-free form (yellow, as seen in the γ complex; see accompanying paper, Jeruzalmi et al., 2001) to the β-bound form (green). The exposure of Phe-74 and Leu-73 in the C-terminal end of helix α4 is balanced by the burial of Trp-61 and Phe-65 in the N-terminal end. The latter residues are exposed in the β-free form, and the structure of the γ complex implicates them in a potential interaction with the δ′ subunit. (D) Model for the open dimeric clamp. The structure of β from the β:δ complex is superimposed twice on one intermolecular interface in the crystal structure of dimeric β (Kong et al., 1992), once using Domain 1 as a reference, and once using Domain 3. A hybrid molecule was then created, which has one open interface and one closed one. Domains 1 and 3 at the closed interface were retained from the crystal structure of dimeric β, whereas the rest of the domains are from the structure of β in the β:δ complex.

clamp loading (Turner et al., 1999). We therefore superimposed the two relaxed forms of β upon Domain I and upon the paired Domain 3 at one interface (the closed one). When this is done, an ~15 Å gap appears at the other interface in the relaxed form of dimeric β (Figure 4D).

The gap in relaxed β is large enough to allow single-stranded DNA to pass into the center of the ring, but is too small for double-stranded DNA. Clamp loading requires double-stranded/single-stranded junctions, or a nick in duplex DNA. Thus, passage of single-stranded DNA into the center of the relaxed β dimer might suffice to allow double-stranded DNA to be threaded into the ring. Alternatively, a slight outward relaxation of the closed interface might allow the gap to widen sufficiently so as to allow double-stranded DNA to enter the ring; interaction with the other subunits of the γ complex (see accompanying paper, Jeruzalmi et al., 2001) may also cause further opening.

Molecular Dynamics Simulations Suggest a Spring-Loaded Component to the Ring Opening Mechanism

We performed two simulations of the nanosecond time-scale dynamics of the β subunit in a solvated environment using standard procedures (for reviews of molecu-

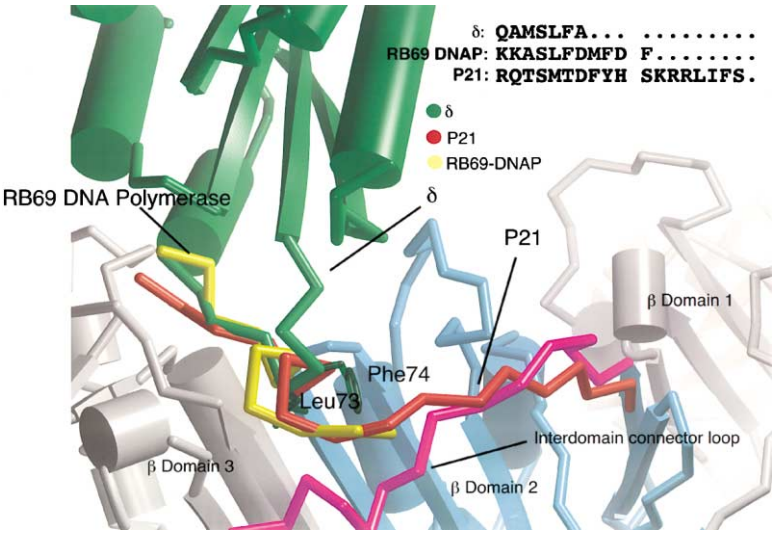

Figure 5. Similarity in the Binding Modes of p21 and RB69 DNA Polymerase to the Interaction of δ with β

The structure of the β subunit in the β:δ complex is shown in gray and cyan. The structures of PCNA complexed to p21 (Gulbis et al., 1996) (PDB code 1AXC) and gp45 of RB69 complexed to a segment of RB69 DNA polymerase (Shamoo and Steitz, 1999) (PDB code 1B8H) were superimposed individually onto the structure of the β subunit by using the β strands at this interdomain interface to overlay the structures. The structure of the p21 peptide (orange) and the RB69 DNA polymerase tethering segment (yellow) are shown, but were not used in the structural superposition. The structure of δ is shown in green. PCNA and gp45 are not shown.

lar dynamics simulations, see Brooks, (1995); Karplus and Petsko, (1991)). In one, we generated a dynamical trajectory for dimeric β, starting from the crystal structure of wild-type dimeric β (Kong et al., 1992). In the other, we started from the same crystal structure of wild-type dimeric β, but we removed one of the two molecules at the start of the trajectory. This allowed us to follow the relaxation of the structure upon removal of the dimer constraints. No artificial driving forces were applied in either trajectory, which were both computed using a standard molecular dynamics procedure for a fully solvated system, using the program AMBER (Cornell et al., 1995; Pearlman et al., 1995). The simulations of dimeric and monomeric β were extended for 2.2 and 3.0 nanoseconds (ns), respectively, and are limited in length by computational resources. For example, the 3 ns simulation of monomeric β required about 45 days of dedicated computer time, using 8 Silicon Graphics R10000 processors.

Dimeric β is stable relative to the crystal structure over the course of the simulation, with both interfaces remaining intact and without a net change in the overall shape of the ring. When all the Cα atoms in the ring are superimposed, the rms deviation in Cα positions with respect to the crystal structure oscillates around ~2.5 Å. In contrast, the simulation of monomeric β produces a remarkable result. Starting from a structure that is identical to that of one monomer in dimeric β, the monomer relaxes within ~1.5 ns to a structure that resembles the more open form of β seen crystallographically in the β:δ complex (Figure 6A). This is illustrated most clearly by superimposing Domain 1 from instantaneous structures in the trajectory onto Domain 1 of the dimeric crystal structure, and then monitoring the rms deviations of Cα atoms in Domain 3 with respect to either Domain 3 in the crystal structure of dimeric β (blue trace in Figure 6B) or β in the crystal structure of the β:δ complex (red trace in Figure 6B). Starting from an rms deviation of 0 Å with respect to Domain 3 of dimeric β, the structure moves away rapidly, and eventually oscillates around an rms deviation of ~10 Å away from Domain 3 in the initial structure. In contrast, Domain 3 in the trajectory is initially ~10 Å away from Domain 3 in the β:δ complex, but relaxes toward it, eventually oscillating around an rms deviation of ~3 Å from the structure in the β:δ complex. The close overlap in the position of Domain 3 in the trajectory with that of the β:δ structure can be readily visualized in Figure 6A.

Large scale conformational changes in proteins are not usually observed on a nanosecond timescale. The rapid structural relaxation in β indicates that the monomer readily adopts a stable and more open structure when not constrained by dimer interactions, without having to surmount large energy barriers. The forces underlying this "spring" are difficult to disentangle. There is no obvious steric effect that caused the domains of β to open up when the dimer restraint is released. The total electrostatic energy of the system undergoes a sharp decrease that correlates with the structural relaxation, but an explanation for this requires further analysis that will be published elsewhere.

RFC-1 Is Likely to Be the Eukaryotic Clamp Loader Subunit that Plays a Role Analogous to δ

The lack of detectable sequence similarity between δ and the subunits of RFC means that sequence comparisons alone cannot reveal which of the 5 RFC subunits is the δ equivalent in eukaryotic clamp loaders. Nevertheless, several points indicate that RFC-1 may be the functional equivalent of δ in the eukaryotic clamp loader system. δ is the only subunit in the clamp loader complex that lacks a Ser-Arg-Cys ("SRC") motif that is conserved in γ and RFC subunits 2 to 5. The arginine side chains of the SRC motifs in δ′ and γ are likely to be crucial for ATP hydrolysis in the adjacent subunits, but the corresponding region of δ does not interact with an ATP binding site (see accompanying paper, Jeruzalmi et al., 2001). δ is also the most divergent of the subunits of the γ complex. This is likely to be a consequence of the lack of a direct function in catalysis, since the generation of proper active site geometry places more stringent requirements on sequence and structure than does the maintenance of protein-protein interfaces alone. Another distinguishing feature of δ is the presence of two

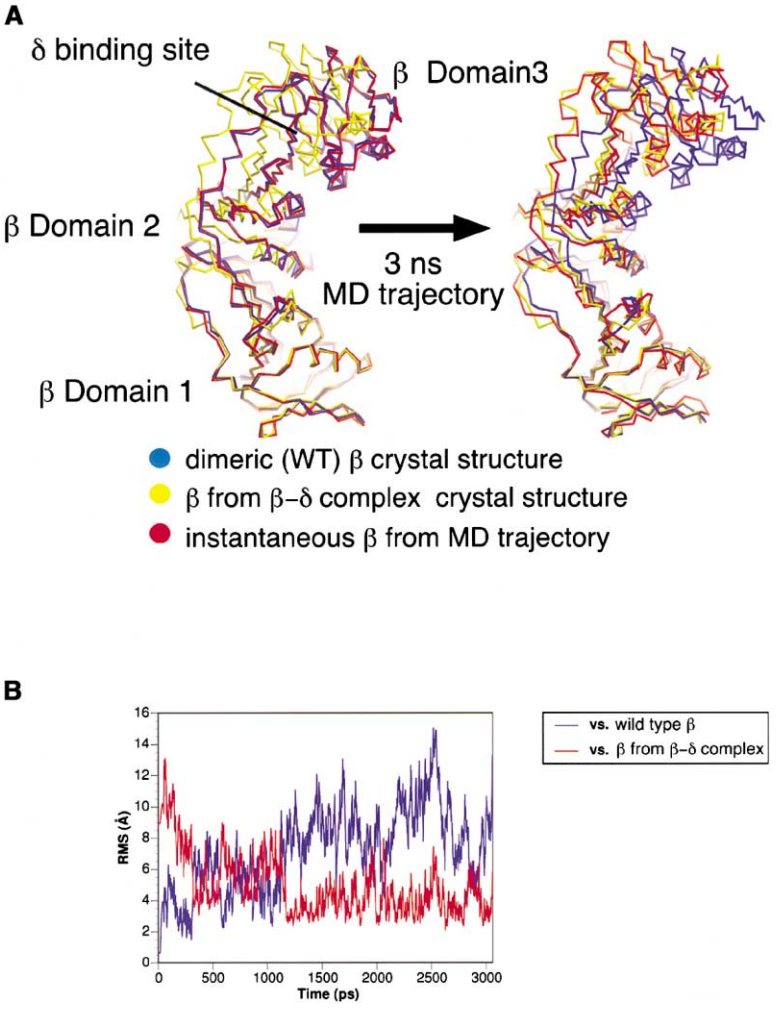

Figure 6. Molecular Dynamics Simulation of the β Subunit

(A) Structures of the β subunit. The backbone structure of one subunit from the dimeric form of β (Kong et al., 1992) (PDB code 2POL) is shown in blue. This structure was used to initiate the molecular dynamics trajectory. The crystal structure of the β monomer in the structure of the β:δ complex is shown in yellow. An instantaneous structure (shown in red) from the start of the trajectory (left) and from the end (right). The structures are superimposed on Cα atoms of Domain 1. (B) Rms deviations in Cα atoms in Domain 3 of β are plotted as a function of time. Instantaneous structures from the trajectory are superimposed on Domain 1 of the reference structure, which is the crystal structure of dimeric β for the blue trace, and the crystal structure of β in the β:δ complex in the red trace.

highly conserved hydrophobic residues, Leu-73 and Phe-74, that form the hydrophobic plug that binds to the surface of β.

RFC-1 is unique amongst the eukaryotic clamp loader subunits in lacking an SRC motif. Also, the eukaryotic RFC-1 sequences appear to form a distinct subgrouping among RFC subunits, and RFC subunits 2–5 are more similar to each other across the span of eukaryotic evolution than they are to RFC-1. A BLAST (Altschul et al., 1990) search of the nonredundant protein database using one of RFC 2–5 readily pulls out sequences of bacterial γ subunits at high confidence levels, while a similar search using RFC-1 does not. Finally, alignment of RFC-1 sequences around the region corresponding to helix α4 in δ and γ reveals a pair of conserved hydrophobic residues (Phe-701 and Tyr-702 in human RFC-1; NCBI accession number P35251) located at a position in the sequence that corresponds to the crucial hydrophobic residues of the bacterial δ subunit. Other RFC subunits do not appear to have a corresponding pair of hydrophobic residues.

These arguments suggest that the δ′ subunit and the three γ subunits of the bacterial γ complex are replaced in the eukaryotic RFC complex by the four closely related RFC subunits 2 to 5. The role of "wrench" is most likely played by RFC-1. Further experiments directed at the interactions between RFC-1 and PCNA are required to test this hypothesis.

Conclusions

The structure of the β:δ complex shows that the clamp loader opens the β ring not by physically pulling apart the two halves of the ring, but rather by trapping one β monomer in a conformation that works against ring closure. The β dimer appears to be held together under some strain, and the interaction with the δ wrench induces or traps conformational changes at the adjacent dimer interface that, in turn, allow the ring to spring open when released.

The similarity in structure between δ and δ′, established by our analysis, extends the evolutionary relationship among clamp loader subunits to include δ. Consideration of structural and sequence features makes it likely that the mechanism described here for ring opening of the β clamp will be similar, at least in general terms, in the eukaryotic RFC/PCNA system. A direct connection to the T4 gp44/gp62/gp45 system is more difficult to make, because the sequence of gp62, like

Table 1. Crystallographic Statistics

β-δ complex (Space group: C2, Cell parameters: a = 200.85 Å, b = 100.15 Å, c = 114.54 Å, α = 90, β = 119.17, γ = 90)

Multiwavelength Dataset	Anomalous Resolution Å	Dispersion Analysis: Reflections (Measured/Unique)	Completeness	R_{sym}[a]	Phasing Power[b]
Se-met (inflection pt: λ = 0.97945) (SBC-APS)	20–4.0	263,821 16,505	99.8	8.6	
Se-met (peak: λ = 0.97931) (SBC-APS)	20–4.0	249,181 16,573	99.9	11.5	0.70
Se-met (low energy: λ = 1.03321) (SBC-APS)	20–4.0	263,657 16,562	99.9	9.5	1.20
Se-met (λ = 0.97931) (High energy: λ = 0.93928) (SBC-APS)	20–4.0	263,019 16,541	99.9	8.5	1.39
Se-met (inflection pt: λ = 0.97940) (NSLS-X25)	20–3.1	592,878 38,316	99.9	14.2	1.20
Se-met (peak: λ = 0.97930) (NSLS-X25)	20–3.5	412,695 23,952	99.9	12.4	0.52
Se-met (λ = 0.97931) (High energy: λ = 0.93928) (NSLS-X25)	20–3.6	390,759 21,713	99.9	13.9	1.16

Overall figure of merit[c]: 0.64 (20–3.5 Å)

Molecular Model Refinement:

β-δ complex (Space group: C2, Cell parameters: a = 198.84, b = 99.29, c = 113.02, β = 119.17)

Dataset	Resolution Å	Reflections (Measured/Unique)	Completeness	R_{sym}[a]
Native (λ = 1.03320) (SBC-APS)	500–2.9	454,054 43,706	98.6	11.0

Reflections |F| > 2σ	Number of Atoms	R_{free}[d] ($R_{working}$[e])	Rmsd (Å) Bonds	Rmsd (°) Angles	Rmsd B Values (Å²) (Main Chain)	(Side Chain)
38,197	10,947	31.07 (25.04)	0.009	1.500	1.543	1.679

Molecular Model Refinement:

β-δ (1-140) complex (Space group: $P_3$21, Cell parameters: a = 110.09 Å, b = 110.09 Å, c = 134.90 Å, α = 90, β = 90, γ = 120)

Dataset	Resolution Å	Reflections (Measured/Unique)	Completeness	R_{sym}[a]
Native (λ = 1.08949) (SBC-APS)	20–2.5	740,503 36,450	98.7	8.0

Reflections |F| > 2σ	Number of Atoms	R_{free}[d] ($R_{working}$[e])	Rmsd (Å) Bonds	Rmsd (°) Angles	Rmsd B Values (Å²) (Main Chain)	(Side Chain)
28,777	3,932	29.42 (24.91)	0.009	1.62	1.620	1.914

[a] $R_{sym} = 100 \times \Sigma|I - \langle I \rangle|/\Sigma I$, where I is the integrated intensity of a given reflection.
[b] Phasing power = $\Sigma|F_H|/\Sigma||F_{PH}(obs)| - |F_{PH}(calc)||$, where F_H is the calculated heavy atom structure factor amplitude.
[c] Figure of merit = $\langle|\Sigma P(\alpha)e^{i\alpha}/\Sigma|P(\alpha)|\rangle$, where α is the phase and P(α) is the phase probability distribution.
[d] $R_{free} = \Sigma|F(obs) - F(calc)|/\Sigma F(obs)$, calculated using 7.6% of the data.
[e] $R_{working} = \Sigma|F(obs) - F(calc)|/\Sigma F(obs)$.

that of δ, is dissimilar to the others, and its structure is as yet unknown.

E. coli β subunit is a particularly stable sliding clamp, with a tight dimer interface and a long half-life on DNA. PCNA from various species is generally less tightly held together as a trimer, and is less stable on DNA than β (Yao et al., 1996). The T4 gp45 clamp is much less stable on DNA, and is likely to be in equilibrium between a closed circular form, visualized in the crystal structures, and various open forms (Alley et al., 2000). Analysis of the γ complex, presented in the accompanying paper (Jeruzalmi et al., 2001), suggests that the disposition of the δ wrench within it is such that an extensive interface between the proximal surface of the ring and the clamp

loader complex is likely. For the less tightly assembled sliding clamps, such an extended interaction might allow the clamp loader to hold the multiple subunits of the clamp together in an open form while the clamp is loaded onto DNA.

Experimental Procedures

Sample Preparation and Characterization

Monomeric β (I272A, L273A; henceforth referred to as β) and δ of *E. coli* were purified from bacterial strains overexpressing them, as described (Dong et al., 1993; Stewart et al., 2001). The β-δ complex was formed by mixing δ with a 5-fold excess of β; uncomplexed β was removed by hydroxylapatite chromatography (BIO-RAD). The N-terminal domain of δ (δ^{1-140}) was overexpressed as a glutathione-S-transferase (GST) fusion protein and purified by chromatography over glutathione sepharose (Pharmacia). δ^{1-140} was released from the GST tag by proteolysis with the tobacco etch virus (TEV) protease at 15°C over 24 hr, followed by mixing with a 5-fold excess of β and resolving the mixture by SourceQ (Pharmacia) chromatography.

Rayleigh light scattering studies of the monomeric β variant and its complex with full-length δ revealed that these species were monodisperse in solution. Multi-angle light scattering studies (Wyatt Technology) yielded a molecular mass of 44.3 kDa for monomeric β that compared well with the expected mass of 40.6 kDa, and a mass of 66–70 kDa for the β-δ complex (expected mass 79.3 kDa).

Crystallization and X-Ray Crystallography

β:δ complexes were dialyzed against 20 mM TRIS-HCl, pH 7.8, 2 mM dithiothreitol, and concentrated to 70 mg/ml (β:δ) or 30 mg/ml (β:δ^{1-140}) by ultrafiltration (Millipore). β:δ crystals (maximum size of ~150 μm^3) grew in 2–3 weeks embedded in a precipitate from solutions containing 70 mg/ml β:δ complex, 100 mM TRIS-HCl, pH 7.5, 975 mM ammonium phosphate at pH 5–6, 4 mM dithiothreitol, 20 mM ammonium tartarate. Crystals of β:δ^{1-140} grew from solutions containing 30 mg/ml β:δ^{1-140}, 50 mM TRIS-HCl, pH 8.0, 10%–11% polyethylene-glycol 4000, 100 mM $MgCl_2$, 2 mM dithiothreitol.

Crystals of β:δ were transferred in steps into solutions containing the final crystallization solution supplemented with 20% glycerol; crystals of β:δ^{1-140} were soaked rapidly (20–30 s) in synthetic mother liquor containing the final crystallization solution supplemented with 20% ethylene glycol. Cryoprotected crystals were shock-cooled in freshly thawed liquid propane for diffraction measurements at −180°C. β:δ crystallized in space group C2 with cell parameters a = 200.9 Å, b = 100.2 Å, c = 114.5 Å, β = 119.17 with 2 copies of the 80 kDa β:δ complex in the asymmetric unit and a solvent content of ~65%. Diffraction data from crystals of β:δ complex were recorded using synchrotron wiggler derived X-radiation (Beamline ID-19, Advanced Photon Source) to Bragg spacings of 2.9 Å. β:δ^{1-140} crystallized in space group $P_3$21 with cell parameters (a = 110.1 Å, b = 110.1 Å, c = 134.9 Å), with a single 56 kDa complex in the asymmetric unit. Native diffraction data were measured to Bragg spacings of 2.5 Å (Beamline ID-19, Advanced Photon Source). In all cases, diffraction data were processed using the HKL package (Otwinowski and Minor, 1997).

Structure Determination, Model Refinement, and Analysis

All attempts to position β or fragments of β from the crystal structure of dimeric β (Kong et al., 1992) by molecular replacement were unsuccessful. Experimental crystallographic phases were obtained using multiwavelength anomalous diffraction (MAD) data recorded around the selenium absorption edge from the 80 kDa β:δ complex, in which β had been labeled with selenomethionine (2 × 15 methionine residues in the asymmetric unit, Table 1). MAD data (20.0–5.0 Å) were used in SOLVE (Terwilliger and Berendzen, 1999) to obtain 11 of 30 Se sites. Density-modified crystallographic phases derived from these sites were used to position both β monomers in the asymmetric unit using a phased translation function. This procedure involved submission of the asymmetric unit of the rotation function (sampled on a 10° grid) through the phased translation function using a single β monomer (derived from the dimeric structure) as a search model. Two peaks above the noise were observed that yielded satisfactory packing of the β molecules in the crystallographic cell. The positioned β monomers allowed the identification of 23 of 30 selenium sites. Experimental MAD phases calculated from these sites were improved using density modification calculations (DM/SOLOMON) including noncrystallographic averaging of electron densities corresponding to the β:δ complexes divided into 6 domains using RAVE (Kleywegt and Read, 1997). Crystallographic computation utilized the CCP4 package (Collaborative Computational Project, 1994).

An electron density map was obtained at 3.1 Å resolution, which allowed interpretation of the structures of both β molecules as well as Domains I and II of δ. Completion of the δ structure utilized a model of δ obtained from the structure of the γ complex (see accompanying paper, Jeruzalmi et al., 2001).

The β-δ^{1-140} structure was solved by molecular replacement using AMORE (Navaza, 1994) using the β monomer and domain I of δ as a search model. The β monomers are located so that a crystallographic axis generates a trimeric ring (reflecting the more open conformation of β in an interesting way) in which Domain 1 of one protomer packs against Domain 3 of another. β is consequently very well ordered in this crystal form, and its overall curvature is the same as that seen in the β:δ crystals, which do not contain a trimeric ring. δ^{1-140} is less well ordered than β, but the regions involved in interaction with β (particularly those residues in helix α4 that are seen to have a drastically different conformation than in the γ complex) have the lowest temperature factors in δ, and are modeled quite reliably.

The β:δ and β:δ^{1-140} models were refined against data to 2.9 Å and 2.5 Å spacings, using ONO (Kleywegt and Jones, 1996) and CNS (Brunger et al., 1998). Refinement made use of both the residual and maximum likelihood refinement targets in CNS. The current β:δ model contains residues 1–366 of β and 1–330 of δ, and displays free and working R values of 31.7% and 25.04%, respectively, against the experimental data. The current β:δ^{1-140} model (residues 1–366 of β and 1–140 of δ) has free and working R values of 29.4% and 24.9%, respectively, against the experimental data. Neither model shows outliers in the Ramachandran plot. Coordinates have been deposited with the Protein Data Bank under the accession codes 1JQJ (β:δ) and 1JQL (β:δ^{1-140})

Molecular Dynamics Simulations

Crystal structures were prepared for dynamics using the Leap module of AMBER (Pearlman et al., 1995). This involved first adding protons to the structure, aligning the principle axes of the protein with the Cartesian axes of the simulation box, and neutralizing the net charge of the protein by adding Na^+ ions. The PARM98 version of the AMBER force field was used (Cornell et al., 1995). All ionizable side-chains were configured in their characteristic ionized states at pH 7.0. All crystallographically determined water positions were retained during the simulation setup. The simulation unit cell was configured as a rectilinear box, which extended 6.0 Å beyond the protein in each dimension. For dimeric β, this resulted in a box size of 107.4 Å × 64.1 Å × 113.1 Å. The protein, crystallographic waters, and ions in the simulation box were then surrounded with water molecules by overlaying a periodic box of waters on top of the crystallographic coordinates and removing any overlapping water molecules. The periodic box of waters (TIP3P water model) (Jorgensen, 1981) had been pre-equilibrated at 298 K via Monte Carlo simulation. Finally, 45 Na^+/Cl^- ion pairs were added at random positions (replacing water molecules in the event of an overlap), such that the molar salt concentration was ~150 mM. The solvated homodimer system contained 60,977 atoms, comprised of 11,410 protein atoms, 22 neutralizing Na^+ ions, 45 Na^+/Cl^- ion pairs, and 16,485 water molecules. Simulations involving monomeric β were set up using the same protocol, resulting in a box size of roughly 75.5 Å × 63.5 Å × 104.7 Å, composed of 38,914 atoms, including 5,705 protein atoms, 11 neutralizing Na^+ ions, 30 Na^+/Cl^- ion pairs, and 11,046 water molecules.

Molecular dynamics trajectories were generated by heating the system to 298 K over a period of 10 picoseconds (ps), followed by equilibration for 50 ps, and then commencing production dynamics at constant temperature and pressure. A distance cutoff of 9.0 Å was used to truncate van der Waals interactions, and particle mesh

Ewald summation (Darden et al., 1995) was employed to eliminate the truncation of electrostatic interactions beyond 9.0 Å.

Acknowledgments

We are grateful to members of the Kuriyan lab for stimulating discussions and for assistance in the measurement of diffraction data. We wish to thank J. Turner, N. Yao, F. Leu for engaging scientific discussions, M. Uy for technical assistance, Benoit Roux for help with the molecular dynamics calculations and L. Leighton for help with illustrations. We are indebted to the scientific staffs of the Advanced Light Source, the Cornell High Energy Synchrotron Source, the National Synchrotron Light Source, the Stanford Synchrotron Radiation Laboratory, the Structural Biology Center, and the Consortium for Advanced Radiation Sources (BioCARS) at the Advanced Photon Source for assistance in the collection of diffraction data. Protein and DNA sequencing was performed by the Protein/DNA Technology Center of the Rockefeller University. Partial support for this work was provided by NIH grants GM R01-45547 (J.K.) and GM R01-38839 (M.O.D.).

Received June 25, 2001; revised July 20, 2001.

References

Alley, S.C., Abel-Santos, E., and Benkovic, S.J. (2000). Tracking sliding clamp opening and closing during bacteriophage T4 DNA polymerase holoenzyme assembly. Biochemistry *39*, 3076–3090.

Altschul, S.F., Gish, W., Miller, W., Myers, E.W., and Lipman, D.J. (1990). Basic local alignment search tool. J. Mol. Biol. *215*, 403–410.

Brooks, C.L., 3rd. (1995). Methodological advances in molecular dynamics simulations of biological systems. Curr. Opin. Struct. Biol. *5*, 211–215.

Brunger, A.T., Adams, P.D., Clore, G.M., DeLano, W.L., Gros, P., Grosse-Kunstleve, R.W., Jiang, J.S., Kuszewski, J., Nilges, M., Pannu, N.S. (1998). Crystallography & NMR system: A new software suite for macromolecular structure determination. Acta Crystallogr. D Biol. Crystallogr. *54*, 905–921.

Collaborative Computational Project, Number 4. (1994). The CCP4 suite programs for protein crystallography. Acta Crystallogr. *D50*, 760–763.

Cornell, W.D., Cieplak, P., Bayly, C.I., Gould, I.R., Merz, K.M., Jr., Ferguson, D.M., Spellmeyer, D.C., Fox, T., Caldwell, J.W., and Kollman, P.A. (1995). A Second Generation Force Field for the Simulation of Proteins, Nucleic Acids, and Organic Molecules. J Am Chem Soc *117*, 5179–5197.

Cullman, G., Fien, K., Kobayashi, R., and Stillman, B. (1995). Characterization of the five replication factor C genes of *Saccharomyces cerevisiae*. Mol. Cell. Biol. *15*, 4661–4671.

Darden, T., York, D., and Pedersen, L. (1995). Particle mesh ewald: An n log(n) method for ewald sums in large systems. J Chem. Phys. *98*, 10089–10092.

Dong, Z., Onrust, R., Skangalis, M., and O'Donnell, M. (1993). DNA polymerase III accessory proteins. I. holA and holB encoding delta and delta′. J. Biol. Chem. *268*, 11758–11765.

Esnouf, R. (1997). An extensively modified version of Molscript that includes greatly enhanced coloring capabilities. J. Mol. Graphics *15*, 133–138.

Flores-Rozas, H., Kelman, Z., Dean, F.B., Pan, Z.-Q., Harper, J.W., Elledge, S.J., O'Donnell, M., and Hurwitz, J. (1994). Cdk-interacting protein 1 directly binds with proliferating cell nuclear antigen and inhibits DNA replication catalyzed by the DNA polymerase δ holoenzyme. Proc. Natl. Acad. Sci. USA *91*, 8655–8659.

Guenther, B.D., Onrust, R., Sali, A., O'Donnell, M., and Kuriyan, J. (1997). Crystal structure of the δ′ subunit of the clamp-loader complex of E. coli DNA polymerase III. Cell *91*, 335–345.

Gulbis, J.M., Kelman, Z., Hurwitz, J., O'Donnell, M., and Kuriyan, J. (1996). Structure of the C-terminal region of $p21^{waf1/cip1}$ complexed with human PCNA. Cell *87*, 297–306.

Hingorani, M.M., and O'Donnell, M. (1998). ATP binding to the Escherichia coli clamp loader powers opening of the ring-shaped clamp of DNA polymerase III holoenzyme. J. Biol. Chem. *273*, 24550–24563.

Hingorani, M.M., and O'Donnell, M. (2000). Sliding clamps: a (tail)ored fit. Curr. Biol. *10*, R25–R29.

Huang, C.-C., Hearst, J.E., and Alberts, B.M. (1981). Two types of replication proteins increase the rate at which T4 DNA polymerase traverses the helical regions in a single stranded DNA template. J. Biol. Chem. *256*, 4087–4094.

Jeruzalmi, D., O'Donnell, M., and Kuriyan, J. (2001). Crystal structure of the processivity clamp loader gamma (γ) complex of E. coli DNA polymerase-III. Cell *106*, this issue, 429–441.

Jorgensen, W.L. (1981). Transferable intermolecular potential functions for water, alcohols and ethers. Application to liquid water. J. Am. Chem. Soc. *103*, 335–340.

Karplus, M., and Petsko, G.A. (1991). Molecular Dynamics Simulations in Biology. Nature *347*, 631–639.

Kelman, Z., and Hurwitz, J. (2000). A unique organization of the protein subunits of the DNA polymerase clamp loader in the archaeon Methanobacterium thermoautotrophicum deltaH. J. Biol. Chem. *275*, 7327–7336.

Kelman, Z., and O'Donnell, M. (1995). DNA polymerase III holoenzyme: Structure and function of a chromosomal replicating machine. Annu. Rev. Biochem. *64*, 171–200.

Kleywegt, G.J., and Jones, T.A. (1996). Efficient rebuilding of protein structures. Acta Crystallogr. D *50*, 829–832.

Kleywegt, G.J., and Read, R.J. (1997). Not your average density. Structure *5*, 1557–1569.

Kong, X.P., Onrust, R., O'Donnell, M., and Kuriyan, J. (1992). Three-dimensional structure of the beta subunit of E. coli DNA polymerase III holoenzyme: a sliding DNA clamp. Cell *69*, 425–437.

Kornberg, A., and Baker, T.A. (1991). DNA Replication, 2 Edition (New York: W.H. Freeman).

Krishna, T.S.R., Kong, X.-P., Gary, S., Burgers, P., and Kuriyan, J. (1994). Crystal structure of the eukaryotic DNA polymerase processivity factor PCNA. Cell *79*, 1233–1243.

Lenzen, C.U., Steinmann, D., Whiteheart, S.W., and Weis, W.I. (1998). Crystal structure of the hexamerization domain of N-ethylmaleimide-sensitive fusion protein. Cell *94*, 525–536.

Leu, F.P., Hingorani, M.M., Turner, J., and O'Donnell, M. (2000). The delta subunit of DNA polymerase III holoenzyme serves as a sliding clamp unloader in Escherichia coli. J. Biol. Chem. *275*, 34609–34618.

Matsumiya, S., Ishino, Y., and Morikawa, K. (2001). Crystal structure of an archaeal DNA sliding clamp: proliferating cell nuclear antigen from Pyrococcus furiosus. Protein Sci. *10*, 17–23.

May, A.P., Whiteheart, S.W., and Weis, W.I. (2001). Unraveling the Mechanism of the Vesicle Transport ATPase NSF, the N-Ethylmaleimide-sensitive Factor. J. Biol. Chem. *276*, 21991–21994.

Moarefi, I., Jeruzalmi, D., Turner, J., O'Donnell, M., and Kuriyan, J. (2000). Crystal structure of the DNA polymerase processivity factor of T4 bacteriophage. J. Mol. Biol. *296*, 1215–1223.

Nakanishi, M., Robetoyre, R.S., Pereira-Smith, O.M., and Smith, J.R. (1995). The C-terminal region of p21SDI1/WAF1/CIP1 is involved in proliferating cell nuclear antigen binding but does not appear to be required for growth inhibition. J. Biol. Chem. *270*, 17060–17063.

Naktinis, V., Onrust, R., Fang, L., and O'Donnell, M. (1995). Assembly of a chromosomal replication machine: two DNA polymerases, a clamp loader, and sliding clamps in one holoenzyme particle. II. Intermediate complex between the clamp loader and its clamp. J. Biol. Chem. *270*, 13358–13365.

Navaza, J. (1994). AMoRe: an automated package for molecular replacement. Acta Crystallogr. A *50*, 157–163.

Neuwald, A.F., Aravind, L., Spouge, J.L., and Koonin, E.V. (1999). AAA+: A class of chaperone-like ATPases associated with the assembly, operation, and disassembly of protein complexes. Genome Res. *9*, 27–43.

Nicholls, A., Sharp, K.A., and Honig, B. (1991). Protein folding and association: insights from the interfacial and thermodynamic properties of hydrocarbons. Proteins Struct. Funct. Genet. *11*, 281–296.

O'Donnell, M., Onrust, R., Dean, F.B., Chen, M., and Hurwitz, J. (1993). Homology in accessory proteins of replicative polymerases - *E. coli* to humans. Nucleic Acids Res. *21*, 1–3.

Onrust, R., Stukenberg, P.T., and O'Donnell, M. (1991). Analysis of the ATPase subassembly which initiates processive DNA synthesis by DNA polymerase. J. Biol. Chem. *266*, 21681–21686.

Otwinowski, Z., and Minor, W. (1997). Processing of X-ray diffraction data collected in oscillation mode. Meth. Enzymol. *276*, 307–326.

Pearlman, D.A., Case, D.A., Caldwell, J.W., Ross, W.S., Cheatham, T.E., III, Fergusen, D.M., Seibel, G.L., Singh, U.C., Weiner, P., and Kollman, P. (1995). AMBER 4.1 (San Francisco, CA: UCSF).

Shamoo, Y., and Steitz, T.A. (1999). Building a replisome from interacting pieces: sliding clamp complexed to a peptide from DNA polymerase and a polymerase editing complex. Cell *99*, 155–166.

Stewart, J., Hingorani, M.M., Kelman, Z., and O'Donnell, M. (2001). Mechanism of beta Clamp Opening by the delta Subunit of Escherichia coli DNA Polymerase III Holoenzyme. J. Biol. Chem. *276*, 19182–19189.

Stillman, B. (1994). Smart machines at the DNA replication fork. Cell *78*, 725–728.

Stukenberg, P.T., Studwell-Vaughan, P.S., and O'Donnell, M. (1991). Mechanism of the sliding β clamp of DNA polymerase III holoenzyme. J. Biol. Chem. *266*, 11328–11334.

Terwilliger, T.C., and Berendzen, J. (1999). Automated MAD and MIR structure solution. Acta Crystallogr. D Biol. Crystallogr. *55*, 849–861.

Tsuchihashi, Z., and Kornberg, A. (1989). ATP interactions of the τ and γ subunits of DNA polymerase III holoenzyme of Escherichia. J. Biol. Chem. *264*, 17790–17795.

Turner, J., Hingorani, M.M., Kelman, Z., and O'Donnell, M. (1999). The internal workings of a DNA polymerase clamp-loading machine. EMBO J. *18*, 771–783.

Waga, S., Hannon, G.J., Beach, D., and Stillman, B. (1994). The p21 inhibitor of cyclin-dependent kinases controls DNA replication by interaction with PCNA. Nature *369*, 574–578.

Warbrick, E., Lane, D.P., Glover, D.M., and Cox, L.S. (1995). A small peptide inhibitor of DNA replication defines the site of interaction between the cyclin-dependent kinase inhibitor p21waf1 and the proliferating cell nuclear antigen. Curr. Biol. *5*, 275–282.

Yao, N., Turner, J., Kelman, Z., Stukenberg, P.T., Dean, F., Shechter, D., Pan, Z.Q., Hurwitz, J., and O'Donnell, M. (1996). Clamp loading, unloading and intrinsic stability of the PCNA, beta and gp45 sliding clamps of human, E. coli and T4 replicases. Genes Cells *1*, 101–113.

Young, M.C., Reddy, M.K., and von Hippel, P.H. (1992). Structure and function of the bacteriophage T4 DNA polymerase holoenzyme. Biochemistry *31*, 8675–8690.

Yu, R.C., Hanson, P.I., Jahn, R., and Brunger, A.T. (1998). Structure of the ATP-dependent oligomerization domain of N- ethylmaleimide sensitive factor complexed with ATP. Nat. Struct. Biol. *5*, 803–811.

Accession Numbers

Coordinates have been deposited with the Protein Data Bank under the accession codes 1JQJ (β:δ) and 1JQL (β:δ^{1-140}).